# Analysis of Fluxless, Reactive Brazing of Al Alloys Using Differential Scanning Calorimetry

STEPHEN FRANCIS CORBIN, SOOKY WINKLER, DENNIS R. TURRIFF, and MARK KOZDRAS

During this investigation, a technique was developed, using differential scanning calorimetry (DSC), to quantitatively analyze the influence of a Ni-based electrolytic braze promotor surface deposit on the furnace brazing of aluminum alloys. The purpose of this braze promoter was to induce a large exothermic surface reaction capable of disrupting a tenacious oxide present on the aluminum braze sheet faying surface. A cyclic DSC methodology was developed which was capable of a quantitative determination of the exothermic reaction ($\Delta H_{exo}$) induced by the Ni plating. Samples with a small quantity of Ni plating exhibited significant "pre-reaction" between Ni and Al in the solid state which resulted in very low $\Delta H_{exo}$ values. Samples with higher quantities of Ni plating exhibited large $\Delta H_{exo}$ values up to 85 kJ/mole.

DOI: 10.1007/s11661-014-2349-3


## I. INTRODUCTION

ALUMINUM and its alloys are extensively used in the aerospace and automotive industries due to their low density, high corrosion resistance, and high specific strength.[1–3] Brazing is an important step in the manufacturing of many aluminum industrial components, including automotive heat exchangers.[1–4] Automotive heat exchangers are commonly produced by joining together an assembly of composite aluminum brazing sheets each having a clad/core-layered structure. The core layer material, which provides strength and the lifecycle requirements of the assembly, typically consists of a AA3000 Al-Mn type alloy. The clad layer uniformly covers both surfaces of the core layer (constituting ~20 pct of the overall braze sheet thickness, 10 pct on each side) and consists of a lower melting point AA4000 Al-Si hypo-eutectic type alloy.[4] During the brazing process, the clad surface acts as the filler metal, thus melting and joining the core sheets together where they are in physical contact.

A principal challenge in Al brazing is the presence of a tenacious oxide film on the faying surface of the braze sheet which can prevent wetting, free flow of the clad layer, and the formation of a defect free metallurgical bond.[3,5] A common way to remove this oxide layer is through the use of controlled atmosphere brazing (CAB) (*e.g.*, the use of a high-purity $N_2$ atmosphere) and the use of a chemical flux such as potassium fluoroaluminate commonly known as NOCOLOK®.[3,5,6] An alternative method that avoids the need for flux is Dana Canada Corporation's proprietary Ni-based fluxless brazing process. CAB, with either the use of NOCOLOK flux or a Ni-based fluxless process, are well established, mass production, commercial methods to produce brazed aluminum components.[3–7] In the fluxless process, a Ni-based braze promoter is electrolytically deposited onto the surface of the Al brazing sheet. Upon heating, oxide penetration is achieved when the Ni reacts exothermically with the underlying Al-rich surface during the brazing process.[7] Qualitatively, the expected mechanisms of the exothermic reaction between an Al brazing sheet and Ni plating have been outlined in Reference 7.

According to the Al-rich corner of the ternary Al-Ni-Si phase diagram (see Figure 1), the presence of Ni at the clad surface and the Si content within the Al-rich clad layer establishes the possibility of Al-Si-Ni ternary eutectic melting at 939 K (565 °C), rather than Al-Si eutectic melting at 850 K ± 1 (577 °C)[8] that would occur in an un-plated braze sheet. This ternary melting event necessarily requires some solid-state reaction between Ni and Al to form $Al_3Ni$, since the ternary melting reaction is $(Al) + (Si) + Al_3Ni = L$. This is a localized event, occurring only at the Ni-plating/clad layer interface. This melting process marks the beginning of a transition zone described by Cheadle and Dockus,[7] where Ni-plating modification and surface oxide disruption occur.

With further heating, the bulk of the clad layer begins to melt and the liquid phase will react fully with the Ni-plating braze promoter to produce an exothermic reaction.[7] It is expected that this exothermic reaction further promotes the disruption of the tenacious oxide

STEPHEN FRANCIS CORBIN, Professor, is with the Department of Civil and Resource Engineering, Dalhousie University, 1360 Barrington Street, P.O. Box 15,000, Halifax, NS B3H 4R2, Canada. Contact e-mail: stephen.corbin@dal.ca SOOKY WINKLER, Manager, is with the Materials & Joining Technology, Dana Canada Corporation, 656 Kerr St., Oakville, ON L6K 3E4, Canada. DENNIS R. TURRIFF, Senior Engineer, is with the MEA Forensic Engineers and Scientists, 226 Britannia Road East, Mississauga, ON L4Z 1S6, Canada. MARK KOZDRAS, Manager, is with the Canmet MATERIALS, Natural Resources Canada, 183 Longwood Road South, Hamilton, ON L8P 0A5, Canada.

Manuscript submitted July 3, 2013.
Article published online May 21, 2014

layer and the promotion of a full metallurgical joint during brazing. Consequently this fluxless brazing process involves the simultaneous thermal events of melting and an exothermic reaction that has yet to be quantitatively measured.

A further aspect during brazing of Al alloys is that the Si within the clad layer diffuses into the Si-deficient core alloy layer. This means that the liquid phase has a transient nature, reducing in volume through diffusional brazing or isothermal solidification (IS) at the brazing temperature.[4] The amount of liquid formed, its duration, and flow during the brazing process are critical for the establishment of a continuous metallurgical bond that is necessary for robust joining and leak integrity of the heat exchanger.[5,9] The role that the Ni braze promoter plays in the diffusional brazing process, including the rate of IS and liquid fraction, is unknown.

Recently,[4] a DSC technique has been developed which was capable of measuring the rate of IS in an un-plated Al braze sheet during a simulated brazing process. One objective of the current work is to further extend the DSC technique to elucidate the reaction mechanisms during brazing in the presence of a Ni-plated braze promoter. A second objective is to measure the rate of IS in a Ni-plated sample. A third objective is to develop an improved understanding of the overlapping exothermic reaction ($\Delta H_{exo}$) and melting events during initial brazing. A fourth objective is to devise a method for quantitative determination of $\Delta H_{exo}$ as a function of Ni-plating weight fraction. Obtaining a direct correlation between the $\Delta H_{exo}$ value and surface oxide disruption is beyond the scope of the current work. However, the methodological developments outlined in this work are an important first step in an ongoing investigation into the details of Ni-Al surface reactions and oxide disruption.

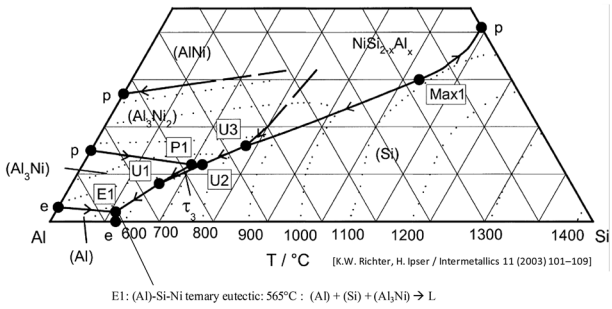


Fig. 1—Liquidus surface of the Al-rich corner of the Al-Ni-Si ternary phase diagram.[22]

## II. MATERIALS AND METHODS

An Al brazing sheet consisting of a modified AA3003 core and AA4045 clad was used for the DSC experiments. Metallographic sections of the as-received brazing sheets revealed an average total sheet thickness of 508 $\mu$m (0.020 in.) where the clad thickness on each side of the braze sheet was approximately 10 pct of the total sheet thickness. The Si-rich clad composition was measured by spark optical emission spectroscopy (OES) on the sheet surface and inductively coupled plasma (ICP) OES. The Si-lean core composition was measured *via* ICP OES after removal of the clad *via* etching. As the results of Table I indicate that the clad and core compositions are similar to AA4045 and AA3003 Al alloys, respectively. The electrolytic deposition of the Ni braze promoter was carried out on some of the Al brazing sheets by Dana Canada Corporation producing four different magnitudes of Ni surface deposit. X-ray fluorescence (XRF) measurements along with metallographic analysis were used to estimate the wt pct of Ni deposited on each of the four braze sheets to be 0.4, 1, 1.5, and 2.0 wt pct, respectively.

Small-round DSC samples (approximately ø 4.76 mm, ≈24 mg mass) were prepared from un-plated and plated sheets using a sample punch. The specimens were then cleaned in acetone and weighed prior to placement in small $Al_2O_3$ crucibles. These were then placed in the DSC for simulated brazing experiments in a dynamic $N_2$ atmosphere (100 mL/min, 99.998 pct pure). All experiments were performed using a temperature and enthalpy-calibrated Netzsch 404C DSC. The initial DSC heating profile involved heating samples up to a nominal brazing temperature of 863 K (590 °C), isothermally holding for a specified time and then interrupting the brazing cycle by cooling back to room temperature (see Figure 2(a)). This interrupted method was then repeated on multiple specimens with increasing brazing hold times. The DSC data were used to quantify the amount of liquid present at the melting and solidification events, in order to determine the rate of isothermal liquid solidification during brazing. During heating, the enthalpy of clad melting was measured through a determination of the area under the melting endotherm peak ($\Delta H_m$, J/g). The enthalpy of solidification was similarly measured during cooling after a specified hold time, $t$ at the braze temperature, to determine the exothermic peak area as a function of brazing time (*i.e.*, $\Delta H_m(t)$). The DSC method is described in more detail elsewhere.[4]

The magnitude of the melting endotherms and solidification exotherms is a measure of the quantity of liquid present in the sample. Therefore, a plot of $\Delta H_m$ as a function of braze time is a measure of the rate of IS.

**Table I. Chemical Composition of the Braze Sheet Clad and Core Layers in Wt Percent (Balance Al)**

| Layer | Cu | Fe | Mg | Mn | Si |
|---|---|---|---|---|---|
| Core | 0.60 | 0.18 | 0.25 | 1.49 | 0.05 |
| Clad | 0.03 | 0.30 | 0.16 | 0.16 | 9.45 |

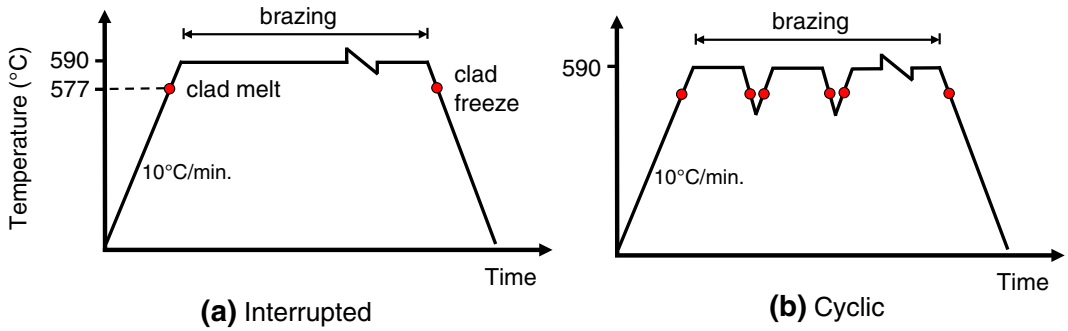


Fig. 2—Schematic illustrations of DSC heating profiles for (*a*) an interrupted method to measure initial melting and solidification after varying hold times for multiple specimens and (*b*) a cyclic method where multiple re-melting and solidification events are captured during successive heating cycles from one specimen.

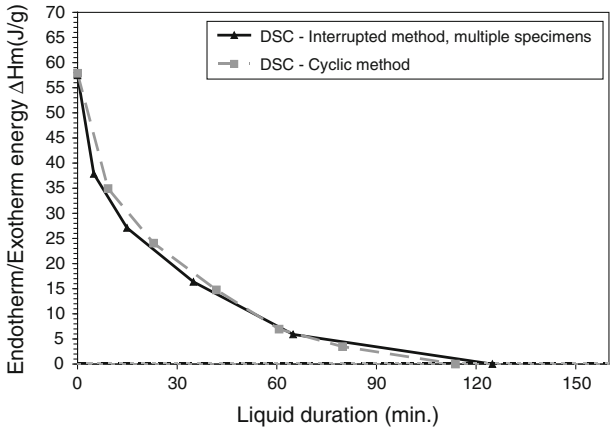


Fig. 3—Comparison of the measured IS rate made from multiple interrupted samples and a cyclic test made on a single No. 12 braze sheet sample.

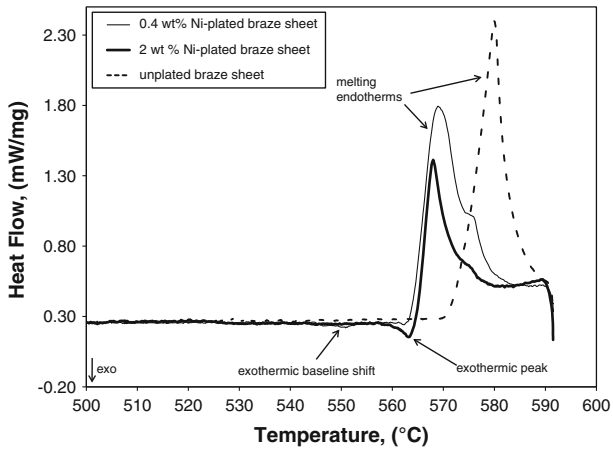


Fig. 4—Initial DSC heating trace for un-plated, low and high wt pct Ni-plated braze sheets.

Such as plot is shown in Figure 3 for a previously studied No. 12 Aluminum braze sheet.[4]

In this previous work,[4] it was indicated that Si diffusion into the core layer during a thermal hold segments below the melting point of the clad layer was negligible. As such, an alternative methodology was developed where a full IS curve could be acquired from a single sample, rather than through the use of a series of separate, interrupted samples. In this cyclic method, a sample was heated up to the nominal brazing temperature of 863 K (590 °C) and held for various times between 1 and 10 minutes. The sample was then cooled to 803 K (530 °C) such that the solidification exotherm could be measured. The sample was then immediately reheated to 863 K (590 °C) and the cycle repeated. The accumulated time above the melting point (*i.e.*, the liquid duration time) was then used as the equivalent isothermal hold time. To compare these methods, Figure 3 plots the IS rate results for both the original interrupted multiple sample method[4] and the cyclic method performed on a single sample of the same type of brazing sheet. This comparison was made as part of the current study using the original No. 12 braze sheet material previously studied.[4] The results indicate that the cyclic method data are in good agreement with that obtained from interrupted samples. As a result, all the DSC experiments reported below used the cyclic DSC method to measure the rate of diffusional solidification.

## III. RESULTS

### A. *Initial Heating and Melting*

Figure 4 presents the initial DSC melting endotherms for an un-plated and two plated Al brazing sheet specimens, one having the highest and the other having the lowest Ni-plating wt pct. The measured onset temperature of the un-plated clad layer melting endotherm is 848 K (575 °C), which closely corresponds to the Al-Si eutectic temperature. The onset of melting for the 0.4 and 2 wt pct Ni-plated samples is 837 K and 838 K (564 °C and 565 °C), respectively, which closely correspond to the Al-Ni-Si ternary eutectic temperature (Figure 1).

For the un-plated sample, the baseline of the DSC trace is flat until melting occurs. In contrast, the plated materials exhibit a small exothermic shift in the baseline, beginning at approximately 803 K (530 °C). In the case of the 2 wt pct plated sample, a distinct exothermic peak develops just before the onset of the melting endotherm. The 1 and 1.5 wt pct plated sample exhibited behavior very similar to the 2 wt pct plated sample.

To further elucidate the nature of the exothermic shift exhibited by the plated material in Figure 4, two separate samples of the 0.4 wt pct plated sheets were heated up in the DSC to temperatures approaching, but not exceeding, the onset of bulk melting [834 K and 836 K (561 °C and 563 °C)]. They were then cooled and their microstructure near the Ni-plating/clad layer interface observed using optical microscopy (see Figure 5). The sample heated to 834 (561 °C) indicates a roughening of the Ni-plating surface compared to the unheated as-plated surface. The phase contrast observable in the optical microscope indicates that the plating layer consists of two phases for the sample cooled from 834 K (561 °C) but progresses to a single phase in the sample cooled from 836 K (563 °C). Also at 836 K (563 °C), the plating layer has grown in thickness and has developed a more significant metallurgical contact and intrusion within the underlying Al-rich clad layer. Some of the intrusion is due to very localized surface melting which was so small in magnitude that it was not measured by the DSC. Chemical analysis using SEM–EDS was not possible on the two distinct phases in the 834 K (561 °C) sample due to their small size. However, the thicker single phase layer in the 836 K (563 °C) sample was confirmed to be $Al_3Ni$. Therefore, the exothermic shift in the baseline of the DSC of Figure 4 is a result of a relatively slow solid-state reaction between Al and Ni to form $Al_3Ni$ as a reaction product, which then becomes a reactant required to allow ternary eutectic melting at 838 K (565 °C) ($Al_3Ni + Si + (Al) \rightarrow L$). Other intermediate intermetallics including AlNi and $AlNi_3$ may also form during this heating stage. The darker contrast in the top layer of the original Ni-plating in Figure 5(a) is expected to be either unreacted elemental Ni or these more Ni-rich intermetallic phases.

An additional observation from the DSC trace of Figure 4 is that the integrated melting endotherm area for the 2 wt pct plated sample ($\Delta H_m$ = 44.99 J/g) is lower in magnitude than the 0.4 wt pct plated sample (75.8 J/g) and the un-plated sample (64.3 J/g). The significance of this observation will be elucidated in Section III–B.

## B. *Diffusional Solidification*

Figure 6 presents the full set of cyclic DSC data for the (a) un-plated and (b) 2 wt pct Ni-plated samples. The initial melting endotherm from Figure 4 is indicated on the graphs with a bolded, dashed gray line. The last cooling segment, after repeated cycling melting/solidification cycles, is also indicated by a dashed black line to distinguish it from the other cycles. There are a number of similarities between the two graphs. Both samples

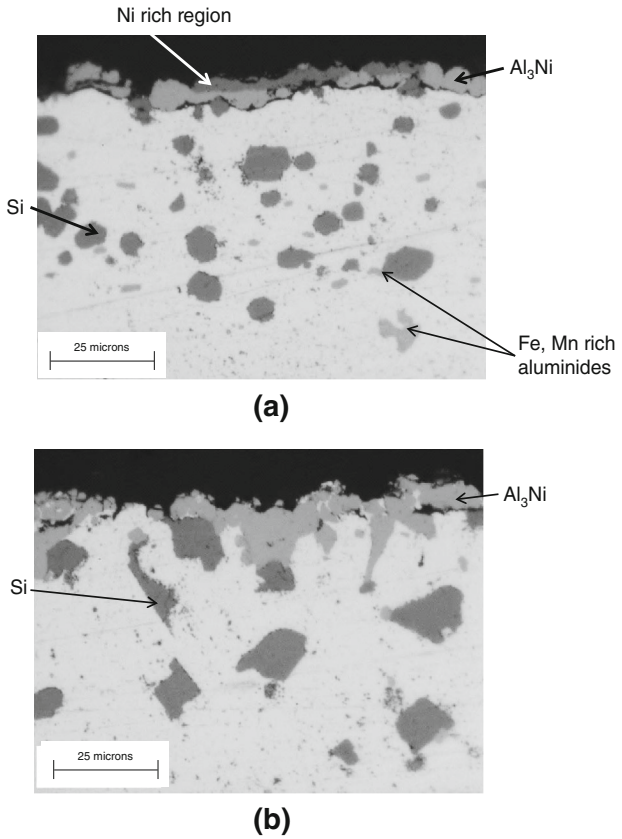


Fig. 5—DSC, 0.4 wt pct samples heated to (*a*) 834 K (561 °C) and (*b*) 836 K (563 °C) and immediately cooled to room temperature.

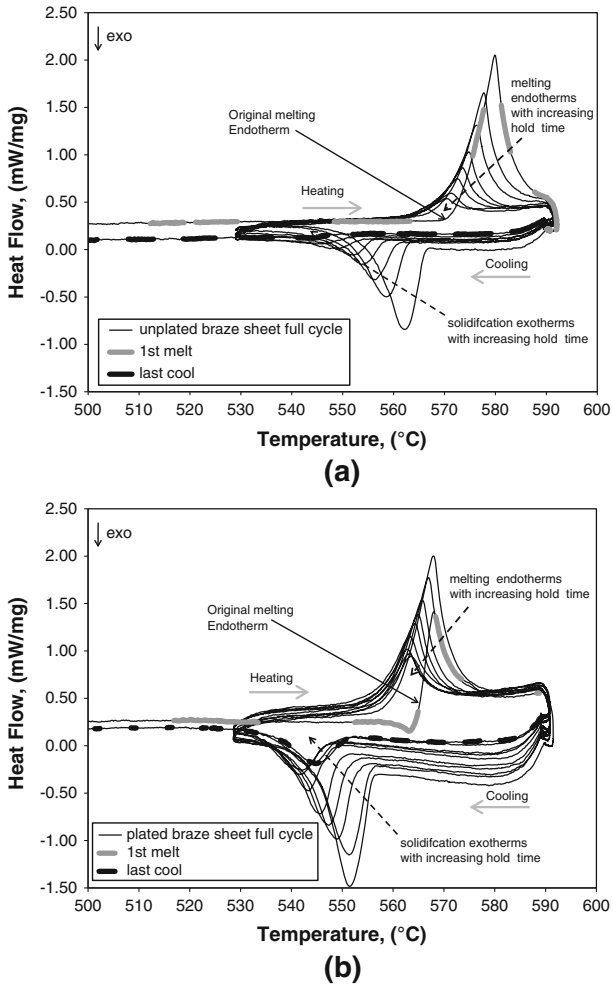


Fig. 6—Full multi-cycle DSC traces for (*a*) un-plated and (*b*) 2 wt pct Ni-plated braze sheets.

indicate a slightly reduced onset temperature of melting during accumulated re-melts compared to the initial melt. However, this onset temperature stabilizes to approximately 842 K (569 °C) in the case of the un-plated sample (which still approximates the Al-Si eutectic temperature) and 831 K (558 °C) for the plated sheet. These onset temperature shifts are expected to be due to a slightly shifted liquid phase composition after initial melt onset, due to both the complete incorporation of Ni into the melt and some dissolution of the core sheet. The most significant alloy element contained within the core and not in the clad is Mn. An introduction of a small amount of Mn into the liquid phase could slightly alter its melting temperature.

A second significant commonality between the cyclic DSC traces in Figure 6 is that both braze sheets indicate a systematic decrease in the size/area of the melting endotherm and solidification exotherms as hold time increases near the braze temperature. This is a clear indication of diffusional removal and solidification of the liquid phase in both the un-plated and plated braze sheets.

There are also some important differences between the un-plated and plated sheet behavior as measured by the DSC. As noted above, the initial endothermic peak in Figure 6(b) during the first melting cycle for the 2 wt pct Ni-plated sheet has a relatively smaller area than that of the un-plated sheet. In fact, this endothermic peak is also lower than the subsequent first cooling exotherm as well as the re-heat (or second) melting endotherm for the plated sample. In contrast, for the un-plated sample in Figure 6(a), the first melting endotherm is the largest, with a systematic decrease in solidification peak and re-melt peak areas over time during the ensuing re-melt cycles. This indicates a continual decrease in the amount of liquid during the brazing process for the un-plated sample.

A second important difference is that, after a liquid duration of ≈220 minutes, complete diffusional solidification of the liquid phase occurs in the un-plated sample. This is evidenced by the lack of a solidification exothermic peak during the last cooling segment/cycle. Conversely, the Ni-plated sample continues to exhibit a solidification exotherm over the brazing times and temperature explored. All the Ni-plated materials exhibited a constant solidification exotherm after 220 minutes of liquid duration, indicating the formation of a persistent liquid phase. The persistent liquid formation is a consequence of the IS behavior of the ternary liquid composition developed in the plated materials. As pointed out by Sinclair and coworkers[10,11] and more recently investigated experimentally[12] for a Ag-Au-Cu ternary system, a ternary liquid composition during IS introduces an additional degree of freedom in the phase equilibria between the solid and liquid phase. This can allow a changing liquid phase composition in the case where one alloying element from the liquid diffuses into the solid more quickly than the other. In the current case, Si is the diffusing species while Ni, with its low solubility in Al remains in the liquid. At the end of the IS process, a phase equilibria is established between the solid phase and a ternary Al-Ni-Si liquid in order to accommodate the lack of solubility of Ni in the Al solid, thus forming a persistent liquid. In a commercial brazing process this influence of Ni on liquid phase formation is not detrimental. This is because some remaining liquid is necessary to form a fillet region near the lap joint. In practice this is achieved through the use of brazing times shorter than 220 minutes and thus avoiding complete IS.

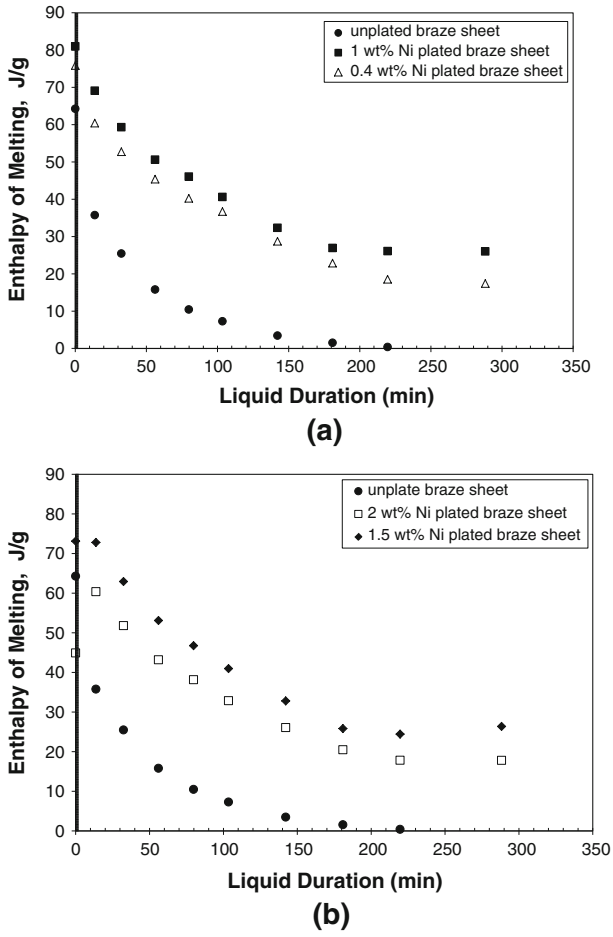


Fig. 7—Enthalpy of melting as a function of liquid duration during brazing (*a*) low wt pct Ni-plated samples and (*b*) high wt pct Ni-plated samples. Data from the un-plated braze sheet are included for comparison.

These two differences were also exhibited by the other Ni-plated samples to a certain degree, as demonstrated in the data of Figure 7. Figures 7(a) and (b) present the melting endotherm and therefore liquid phase present/remaining within the braze sample, as a function of brazing hold time or liquid duration starting from the melt onset time. The data of Figure 7 are an average of three separate cyclic experiments. The standard deviation in the melting enthalpy measurements was in the range of 2.7 to 4.7 pct.

Figure 7(a) shows that the melting endotherm or liquid volume present in the un-plated braze sheet rapidly decreases, particularly at the early stages of brazing. The rate of diffusional solidification in the sample is such that, after a liquid duration time of 220 minutes, complete diffusional solidification has

occurred at the brazing temperature and no liquid remains upon cooling (*i.e.*, 0 J/g for enthalpy). The 2 wt pct Ni-plated sheet (*i.e.*, Figure 7(b)) indicates a relatively lower initial melting endotherm, which is actually lower than the melting endotherm at the ensuing data point of 14 minutes. This is in sharp contrast to the un-plated sample which exhibits a liquid reduction of 45 pct after 14 minutes. The other plated samples show similar trends to the 2 wt pct Ni sample, with either the same melting endotherm present after 14 minutes (*i.e.*, the 1.5 wt pct Ni-plated sample) or only small reductions of 10 and 15 pct for the 1 and 0.4 wt pct Ni-plated samples, respectively. It is proposed that the reason for the lower initial melting endotherm in the plated samples is due to overlapping, opposing thermal events: the endothermic process of melting and the simultaneous exothermic reaction between Al and the Ni plating. Therefore, the initial melting endotherm for the plated materials is only apparent and leads to complications in quantification *via* DSC.

The Al-Ni exothermic reaction is a one-time, non-reversible reaction. Figure 6(a) shows that with subsequent re-heating and cooling cycles, only the melting event re-occurs. Without the attenuating influence of the exothermic reaction, the melting endotherm increases in the subsequent cycles to its actual values, rather than the apparent value exhibited in the first melting cycle. In Figure 7, the braze sheet with the thickest Ni plating exhibits the lowest initial apparent melting endotherm, indicating that it also exhibited the largest irreversible Al-Ni exothermic reaction due to the increased amount of Ni.

To provide further evidence of this phenomenon, samples were heated to only 843 K or 863 K (570 °C or 590 °C) within the DSC, immediately cooled and their microstructures observed. From the DSC trace of Figure 4, it is clear that cooling from 843 K (570 °C) would interrupt the full melting process in the clad layer of the Ni-plated braze sheets. Conversely, cooling from 863 K (590 °C) allows for liquation of the clad layer. Figures 8 and 9 present the microstructural results of these interrupted tests for the 0.4, 1, and 2 wt pct Ni-plated samples.

Figure 8 indicates that an increase in Ni-plating wt pct results in a greater disruption and interaction with the original Ni surface plating, as evidenced by an increased volume fraction of $Al_3Ni$ dispersed within the clad layer. In the 0.4 and 1 wt pct plated samples, the $Al_3Ni$ phase is primarily distributed near the surface of the clad layer, while this phase is dispersed through most of the clad thickness in the 2 wt pct plated sample. The $Al_3Ni$ phase is the main product of the exothermic reaction $Al + Ni \rightarrow Al_3Ni$. Therefore, Figure 8 provides strong evidence of a more significant exothermic

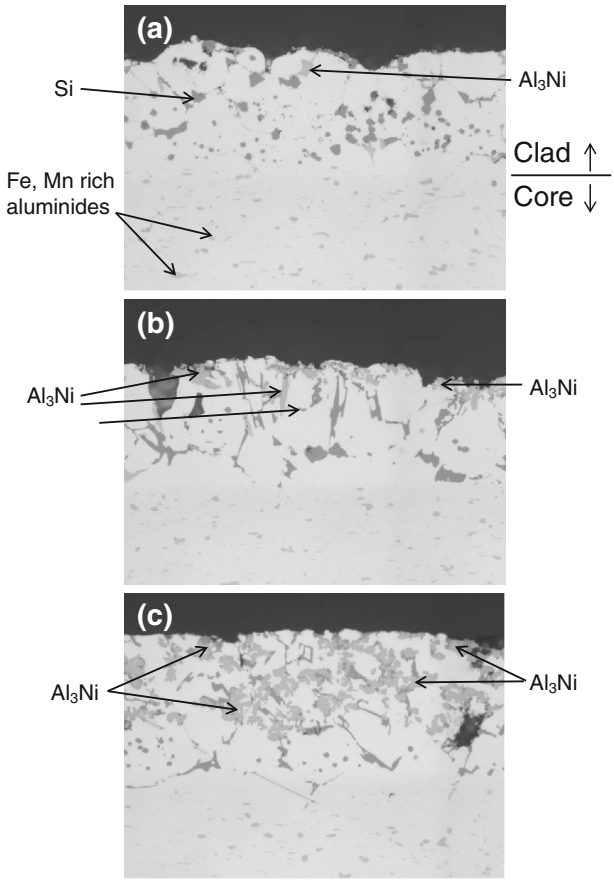


Fig. 8—Microstructures of (*a*) 0.4 wt pct, (*b*) 1 wt pct, and (*c*) 2 wt pct Ni-plated samples cooled from 843 K (570 °C).

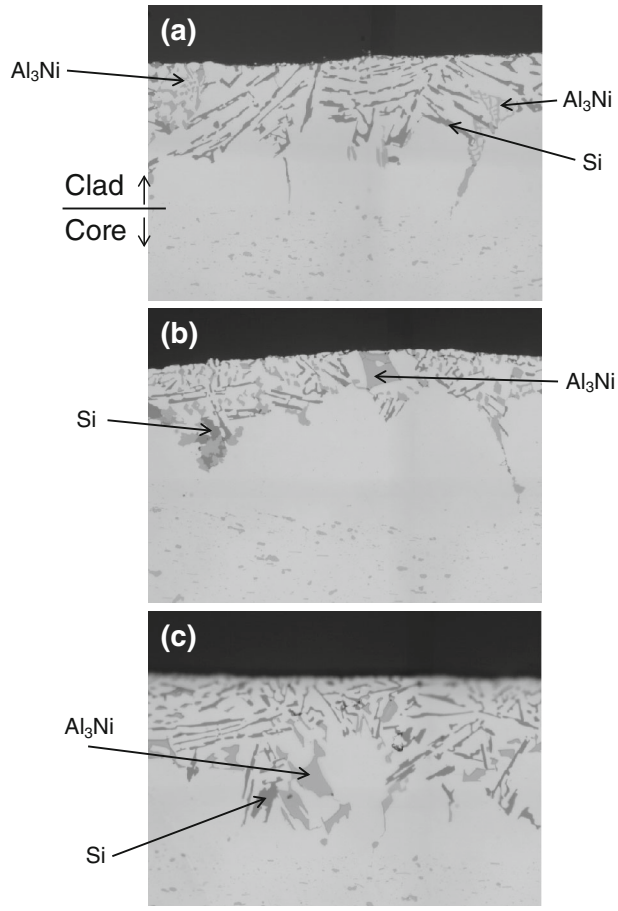


Fig. 9—Microstructures of (*a*) 0.4 wt pct, (*b*) 1 wt pct, and (*c*) 2 wt pct Ni-plated samples cooled from 863 K (590 °C).

reaction occurring in the thicker plated samples and that this reaction precedes and overlaps with the clad melting process.

Figure 9 indicates that full melting (followed by cooling) promotes a well-developed ternary eutectic microstructure consisting of the (Al), (Si), and $Al_3Ni$ phases. Comparison of Figures 8 and 9 indicates that the Ni-plating wt pct has less influence over the microstructure once a full liquid phase is developed. This supports the above finding that the exothermic reaction is a one-time non-reversible event, after which a stable melting and re-solidification process is established during the cyclic DSC experiments. Concomitant diffusional solidification taking place during the brazing process then determines the liquid volume present as a function of brazing time.

As shown in a previous study for un-plated Al brazing sheet No. 12,[4] as well as other aluminum brazing studies,[5,9] the diffusion of Si from the Si-rich liquated clad layer into the Si-deficient core causes a mass-flux imbalance across the solid–liquid interface. As Si diffuses into the α(Al) core, the solid–liquid interface gradually migrates outwards as the α(Al) grains grow epitaxially into the liquid. The volume of eutectic, or off-eutectic Al-Si liquid necessarily decreases over time, as evidenced by DSC. The remaining Si-rich liquid is typically located near the clad surface and at the inter-dendritic locations between the growing primary α(Al) grains, as found in Reference 4 and shown here in Figure 9.

## IV. ANALYSIS

Comparison of Figures 7(a) and (b) shows that all Ni-plated braze sheet materials have a similar rate of IS. As pointed out in previous work,[13,14] both the rate of IS and the completion time are dependent on the underlying diffusional mechanisms that determine the solidification process. For the materials of study here, this is the diffusion of Si from the liquid phase into the low Si content core layer. The trends of Figure 7 indicate that the presence of a Ni plating does not significantly alter the overall mechanism of IS.

It has been shown that the process of IS at a planar solid–liquid interface (*e.g.*, during transient liquid phase bonding) proceeds at a rate that is parabolic with time.[13–15] In this previous work, the base material is considered to be semi-infinite in dimension. In the current case, the base material or core layer has a finite size, which could cause a deviation from a parabolic rate dependence, particularly at longer hold times. However, an estimate of the rate of IS was still possible assuming a parabolic time dependence as illustrated in Figure 10. Plotting the melting endotherm as a function of the square root of time does result in a linear trend for the rate of IS. Note that the initial melting peak, which is only apparent, due to the overlapping exotherm and endotherm, and the data during the persistent liquid phase stage, is not included in the plot. Table II presents the results of linear regression analysis of the data of Figure 10. The linear regression line for the 2 wt pct plated braze sheet is included in the plot of Figure 10 as well as the initial, apparent melting endotherm measurement for comparison purposes.

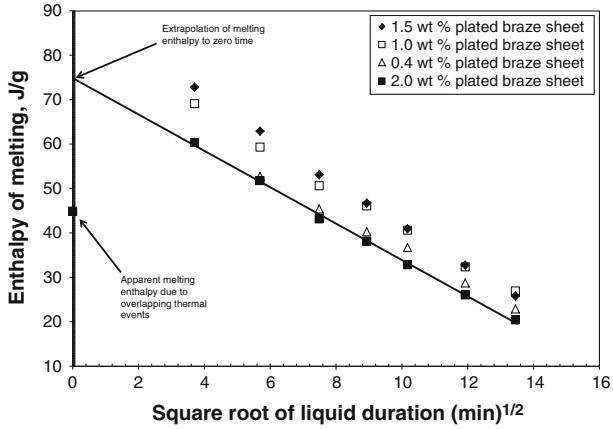


Fig. 10—Enthalpy of melting in the plated braze sheets as a function of the square root of time.

The high correlation coefficient for the linear regression indicates that the rate of IS is well described as parabolic with time. The slope (or rate constant) for the regression lines for all 4 Ni-plated samples is similar, ranging between −3.81 and −4.81, indicating that the diffusional mechanism responsible for all four Ni-plated sheets is the same, as would be expected.

Using the linear regression analysis allows an extrapolation of the data back to zero time and an estimate of the initial enthalpy of melting present ($\Delta H_{melt}$), which overlaps with the exothermic reaction ($\Delta H_{exo}$) occurring between the Ni-plating and the Al clad layer. These values are indicated in the intercept column of Table II and range between 74.5 and 90 J/g.

An estimate of the actual exothermic reaction ($\Delta H_{exo}$) introduced by the Ni plated can now be determined by assuming that the exothermic and melting reactions subtract from each other, giving rise to the measured apparent melting ($\Delta H_{meas}$) enthalpy at zero time by the DSC;

$$\Delta H_{meas} = \Delta H_{melt} - \Delta H_{exo}, \quad [1]$$

or

$$\Delta H_{exo} = \Delta H_{melt} - \Delta H_{meas}. \quad [2]$$

The results of such a calculation are given in column 4 of Table III. The calculations indicate that the magnitude of the exothermic reaction increases as the Ni-plating wt pct increases.

The exothermic energy calculated in column 4 of Table III is based on the entire sample weight. Using the estimated Ni-plating wt pct measured from the XRF method, the exothermic energy can be expressed in terms of the moles of Ni present on the sample. The results of this calculation are given in column 5 of Table III. The exothermic energy is as high as 85 kJ/mole, indicating that the reaction introduced by the Ni plating is highly exothermic providing that the plating wt pct is sufficient.

Table II. Results for Linear Regression Analysis of the IS Rate for Ni-Plated Braze Sheets

| Material | Slope | Intercept | Correlation Coefficient |
|---|---|---|---|
| 0.4 wt pct Ni-plated braze sheet | −3.817 | 74.51 | 0.9985 |
| 1 wt pct Ni-plated braze sheet | −4.299 | 84.13 | 0.9974 |
| 1.5 wt pct Ni-plated braze sheet | −4.8132 | 90.08 | 0.9990 |
| 2.0 wt pct Ni-plated braze sheet | −4.095 | 74.88 | 0.9982 |

Table III. Enthalpy Measurements and Estimates for the Apparent Melting Endotherm ($\Delta H_{meas}$), the Predicted Melting Endotherm ($\Delta H_{melt}$), and the Calculated Exotherm ($\Delta H_{exo}$) for the First Peak Measure on the DSC Trace for the Four Ni-Plated Braze Sheets of This Study

| Material | $\Delta H_{meas}$ (J/g) | $\Delta H_{melt}$ (J/g) | $\Delta H_{exo}$ (J/g) | $\Delta H_{exo}$ Ni Content (kJ/mole) |
|---|---|---|---|---|
| 0.4 wt pct Ni-plated braze sheet | 75.8 | 74.5 | ≈0 | 0 |
| 1 wt pct Ni-plated braze sheet | 81.0 | 84.1 | 3.1 | 17.6 |
| 1.5 wt pct Ni-plated braze sheet | 73.1 | 90.1 | 17 | 65.2 |
| 2.0 wt pct Ni-plated braze sheet | 44.9 | 74.9 | 30 | 85.8 |

The reaction (or combustion synthesis) of Ni and Al to form various nickel-aluminides has been extensively studied by others.[16–21] The case of fluxless brazing using a Ni-based braze promoter, closely resembles the thermal explosion mode of combustion synthesis. This involves placing the reactants in contact and heating them until a large exothermic reaction initiates. The sequence of events during heating involves some "pre-combustion" where a solid-state growth of $Al_3Ni$ forms at the Ni-Al interface.[17] With further heating, the large exothermic reaction is initiated by the formation of a liquid phase, due to the eutectic reaction $Al + Al_3Ni = L$ in the case of binary Ni-Al. In the current case, with the presence of Si, the ternary form of the eutectic reaction results in liquid formation.

The next sequence of events results from the interaction between the Al-rich liquid and Ni. A number of reactions are possible, forming $Al_3Ni_2$, AlNi, or $AlNi_3$. Interpreting the exothermic energy of this multiple step reaction is difficult. The heat required to form $Al_3Ni$, $Al_3Ni_2$, AlNi, or $AlNi_3$ is reported to be in the range between 38 and 112 kJ/mole.[14–18] Given the complexity of the reaction, the range of exothermic energies reported in column 4 of Table III agrees well with those reported in the literature.

The decrease in the exothermic energy, on a Ni mole fraction basis, as a function of Ni-plating wt pct, is due to the influence of the "pre-combustion" in the solid state. Any formation of $Al_3Ni$ in the solid state will reduce the magnitude of the exothermic reaction taking place upon melting, by reducing the presence of the pure Ni reactant. If all the Ni "pre-reacts" to form $Al_3Ni$ in the solid state, then no exothermic reaction upon melting would be expected. The microstructural analysis of Figure 5 indicates that all the Ni does pre-react in the case of the Ni-plated braze sheet with a 0.4 wt pct Ni plating. This is consistent with the DSC analysis of Figure 10 and calculations of Table III which indicate a near zero exotherm for the 0.4 wt pct Ni-plated sheet. With an increase in the Ni-plating wt pct, relatively more Ni remains after the "pre-combustion" stage and initiates a larger exothermic reaction upon melting.

## V. CONCLUSIONS

During this investigation the rate of IS of an Al-Si clad layer with and without a Ni plating, indicated that the underlying diffusional mechanisms responsible for the rate of IS were similar. Despite this similarity, the Ni-plated braze sheets exhibited smaller initial melting endotherms compared to the un-plated material. The magnitude of this melting endotherm decreased as the Ni-plating wt pct increased. This smaller endotherm was interpreted to be due to overlapping exothermic and endothermic peaks resulting from the simultaneous exothermic reaction between Ni and liquid Al at the braze sheet surface and bulk melting of the Si-rich filler layer.

A full analysis of the results leads to the conclusion that the DSC can be used to quantitatively analyze the IS phenomena which occurs during furnace brazing of aluminum sheets. It can further be used to deconvolute overlapping exothermic and endothermic events induced by the presence of a Ni plating. This allows an analysis of the effectiveness of the Ni plating in developing a large exothermic reaction at the braze sheet surface.

## ACKNOWLEDGMENTS

The authors would like to gratefully acknowledge the important financial support of the National Sciences and Engineering Research Council of Canada (NSERC), the Initiative for Automotive Manufacturing Innovation (IAMI), and the financial and in-kind contribution of Dana Canada Corporation, Oakville, ON. They would also like to thank Peirre Marois at

the Novelis Global Technology Centre (NGTC) for his assistance in braze sheet chemical analysis.

## REFERENCES


1. W.S. Miller, L. Zhuang, J. Bottema, A.J. Wittebrood, P. De Smet, A. Haszler, and A. Vieregge: *Mater. Sci. Eng. A*, 2000, vol. A280, pp. 37–49.
2. J. Zahr, S. Oswald, M. Turpe, H.J. Ullrich, and U. Fussel: *Vacuum*, 2012, vol. 86, pp. 1216–18.
3. G. Zhang, Y. Bao, Y. Jiang, and H. Zhu: *J. Mater. Eng. Perform.*, 2011, vol. 20, pp. 1451–56.
4. D.M. Turriff, S.F. Corbin, and M. Kozdras: *Acta Mater.*, 2010, vol. 58, pp. 1332–41.
5. D.P. Sekulic: *Int. J. Eng. Sci.*, 2001, vol. 39, pp. 229–41.
6. G.J. Marshall, R.K. Bolingbroke, and A. Gray: *Metall. Trans. A*, 1993, vol. 24A, pp. 1935–42.
7. B.E. Cheadle and K.F. Dockus: *Inert Atmosphere Fluxless Brazing of Aluminum Heat Exchangers*, SAE Technical Paper 880446, 1988, DOI:10.4271/880446.
8. T.B. Massalski: in *Binary Alloy Phase Diagrams*, American Society for Metals (ASM) International, Metals Park, OH, 1990.
9. J. Lacaze, S. Tierce, M.C. Lafont, Y. Thebeault, N. Pébère, G. Mankowski, C. Blanc, H. Robidou, D. Vaumousse, and D. Daloz: *Mater. Sci. Eng. A*, 2005, vols. A413–A414, pp. 317–21.
10. C. Sinclair: *J. Phase Equilib.*, 1999, vol. 20, pp. 361–69.
11. C. Sinclair, G. Purdy, and J. Morral: *Metall. Mater. Trans. A*, 2001, vol. 31A, pp. 1187–92.
12. M.L. Kuntz, B. Panton, S. Wasiur-Rahman, Y. Zhou, and S.F. Corbin: *Metall. Mater. Trans. A*, 2013, vol. 44A, 3708–20.
13. M. Kuntz, N. Zhou, and S.F. Corbin: *Metall. Mater. Trans. A*, 2006, vol. 37A, pp. 2493–2504.
14. M. Kuntz, S.F. Corbin, and N. Zhou: *Acta Mater.*, 2005, vol. 53, pp. 3071–82.
15. Y. Zhou, W.F. Gale, and T.H. North: *Int. Mater. Rev.*, 1995, vol. 40, pp. 181–96.
16. A. Biswas and S.K. Roy: *Acta Mater.*, 2004, vol. 52, pp. 257–70.
17. A. Biswas, S.K. Roy, K.B. Gurumurthy, N. Prabhu, and S. Banerjee: *Acta Mater.*, 2002, vol. 50, pp. 757–73.
18. F.Z. Chrifi-Alaoui, M. Nassik, K. Mahdouk, and J.C. Gachon: *J. Alloys Compd.*, 2004, vol. 364, pp. 121–26.
19. R. Pretorius, R. De Reus, A.M. Vredenberg, and F.W. Saris: *Mater. Lett.*, 1990, vol. 9, p. 494.
20. X. Qiu and J. Wang: *Scripta Mater.*, 2007, vol. 56, pp. 1055–58.
21. X. Qiu, J. Zhu, J. Olier, C. Yu, Z. Wang, and H. Yu: *J. Phys. D Appl. Phys.*, 2009, vol. 42, pp. 1–6.
22. K.W. Richter and H. Ipser: *Intermetallics*, 2003, vol. 11, pp. 101–09.